



ELSEVIER

Contents lists available at ScienceDirect

Solid State Ionics

journal homepage: [www.elsevier.com/locate/ssi](http://www.elsevier.com/locate/ssi)

## Structure analyses of Fe-substituted Li<sub>2</sub>S-based positive electrode materials for Li-S batteries

Tomonari Takeuchi<sup>a,\*</sup>, Hiroyuki Kageyama<sup>b</sup>, Noboru Taguchi<sup>a</sup>, Koji Nakanishi<sup>c</sup>, Tomoya Kawaguchi<sup>b</sup>, Koji Ohara<sup>d</sup>, Katsutoshi Fukuda<sup>b</sup>, Atsushi Sakuda<sup>a</sup>, Toshiaki Ohta<sup>c</sup>, Toshiharu Fukunaga<sup>b</sup>, Hikari Sakaebe<sup>a</sup>, Hironori Kobayashi<sup>a</sup>, Eiichiro Matsubara<sup>b</sup>

<sup>a</sup> National Institute of Advanced Industrial Science and Technology (AIST), Midorigaoka 1-8-31, Ikeda, Osaka, 563-8577, Japan

<sup>b</sup> Office of Society-Academia Collaboration for Innovation, Kyoto University, Uji, Kyoto 611-0011, Japan

<sup>c</sup> Synchrotron Radiation Center, Ritsumeikan University, 1-1-1 Noji-Higashi, Kusatsu, Shiga 525-8577, Japan

<sup>d</sup> The Research & Utilization Division, Japan Synchrotron Radiation Research Institute (JASRI), 1-1-1 Kouto, Sayo, Hyogo 679-5198, Japan

### ARTICLE INFO

#### Keywords:

Fe-substituted lithium sulfide  
Low crystalline material  
Lithium sulfur battery  
Pair distribution function analysis  
High capacity

### ABSTRACT

The structure of Fe-substituted Li<sub>2</sub>S-based positive electrode material Li<sub>8</sub>FeS<sub>5</sub> was analyzed using high-energy X-ray total scattering measurements. Pair distribution function (PDF) analyses indicated that the mechanically milled Li<sub>8</sub>FeS<sub>5</sub> sample could best be described as having an anti-fluorite structure in which Fe ions partially occupy Li sites in the *Fm $\bar{3}$ m* unit cell. The electrochemical properties of a cell utilizing Li<sub>8</sub>FeS<sub>5</sub> as the positive electrode were also consistent with this structural model.

### 1. Introduction

Recently, there is an increasing demand for high energy storage systems, particularly utilized in electric vehicles, and there requires next generation battery system with much higher energy density than currently available lithium-ion battery with oxide-based cathodes (theoretically *ca.* 500 Wh·kg<sup>-1</sup>, practically *ca.* 200 Wh·kg<sup>-1</sup>) [1–3]. Among them, lithium-sulfur cell is one of the potential alternative battery systems to generate high energy density (theoretically *ca.* 2600 Wh·kg<sup>-1</sup>). Lithium sulfide (Li<sub>2</sub>S) is a promising cathode material for Li-S cell with high theoretical capacity (*ca.* 1170 mAh·g<sup>-1</sup>) and can be used with a variety of anode materials (such as graphite, silicon) in practical battery systems [4–17]. However, this material shows high electrical resistivity, which gives rise to poor material utilization in the cells. In order to enhance the conductivity of Li<sub>2</sub>S, several attempts, such as forming composites with metals (Li<sub>2</sub>S-Fe, Li<sub>2</sub>S-Cu) [4–6] or carbon (Li<sub>2</sub>S-C) [7–12], have been performed. Recently, we prepared Li<sub>2</sub>S-FeS<sub>x</sub> (*x* = 1, 2) composites using a combination of thermal heating and mechanical milling [15]. The composites consisted of Fe-containing low-crystalline Li<sub>2</sub>S and showed relatively high specific capacity in the case of the Li<sub>2</sub>S-rich composition, typically *ca.* 730 mAh·g<sup>-1</sup> for the 4Li<sub>2</sub>S-FeS composite (Li<sub>8</sub>FeS<sub>5</sub>) cell. Although relatively high discharge capacity was attained, the detailed structure of Li<sub>8</sub>FeS<sub>5</sub> itself is still unclear. Clarifying the structure of Li<sub>8</sub>FeS<sub>5</sub> is necessary for

understanding the charge/discharge mechanism, as well as for designing Li<sub>2</sub>S-based electrodes with higher electrochemical performance.

In the present work, we have analyzed the structure of Li<sub>8</sub>FeS<sub>5</sub> using X-ray diffraction and scattering measurements, particularly in the course of its preparation (mechanical milling) in an attempt to trace the atomic re-arrangements during mechanochemical treatment.

### 2. Experimental

An Li<sub>8</sub>FeS<sub>5</sub> sample was prepared as reported previously [15]: a blended powder of Li<sub>2</sub>S and FeS in a 4:1 M ratio underwent spark plasma sintering (SPS; SPS-3.20 MK-IV, Fuji Electronic Industrial, Japan) at 600 °C for 3 min under an argon atmosphere, and the product (hereafter referred to SPS(600 °C)) was blended with acetylene black (AB) powder in a 9:1 weight ratio, and then mechanically milled for 8 h using a pulverizer [18] (Model No. MC-4A, Ito Seisakusho Ltd., Japan) at a rotation speed of 1000 rpm. During the milling process, small amounts of powder were extracted at given intervals for sample characterization, and these powders were labelled MM(*t*), where *t* was the time after commencing milling, namely, 0 h, 0.5 h, 1 h, 2 h, and 8 h. Since Li<sub>2</sub>S and Li<sub>8</sub>FeS<sub>5</sub> are very sensitive to atmospheric moisture, all the procedures except for the SPS and mechanical milling were carried out in an argon-filled glove box; the SPS and mechanical milling were carried out under the atmospheric condition using the argon-filled

\* Corresponding author.

E-mail address: [takeuchi.tomonari@aist.go.jp](mailto:takeuchi.tomonari@aist.go.jp) (T. Takeuchi).

container and pot wherein  $\text{Li}_2\text{S}$  and  $\text{Li}_8\text{FeS}_5$  were enclosed, and all the other procedures, such as powder blending and grinding, were carried out in an argon-filled glove box.

Phase purity of the samples was checked by X-ray diffraction (XRD) (RINT TTR-III, Rigaku, Japan) using monochromatic  $\text{Cu K}\alpha$  radiation within a  $2\theta$  range of  $10 - 125^\circ$ . Before the measurements, each sample was covered with Kapton film in an argon-filled glove box, and measurements were carried out within 1 h to minimize reaction with atmospheric moisture. Structural refinement by X-ray Rietveld analysis was carried out using the RIETAN-2000 program [19]. Morphologies of each sample were examined using a scanning electron microscope (SEM; JEOL JSM-5500LV). The local atomic structure of each sample powder was examined by taking high-energy X-ray total scattering measurements, which were carried out at BL28XU of SPring-8 [20]. The incident X-ray energy was 38.0 keV, and scattering patterns measured with a  $Q$ -range from 0.3 to  $17 \text{ \AA}^{-1}$  were analyzed using pair distribution function (PDF) analyses [21–24]. A vacuum chamber was used to avoid air scattering the sample. The measured datasets were corrected for absorption, background, and polarization effects, and were normalized to obtain the reduced pair distribution function  $G(r)$ , according to the procedure detailed elsewhere [22].

Electrochemical lithium insertion/extraction reactions were carried out using lithium coin-type cells. The working electrode consisted of a mixture of 11.1 mg of the  $\text{Li}_8\text{FeS}_5$  composite (containing 10% (1.1 mg) AB) and 3.9 mg of additional AB powder with 0.5 mg of Teflon powder pressed into a 15 mm diameter tablet under a pressure of 10 MPa. The electrochemical test cell was constructed in a stainless steel coin-type configuration. The negative electrode was a 15 mm diameter and 0.2 mm thick disk of Li foil, and the separator was a microporous polyolefin sheet. A solution of 1 M  $\text{LiPF}_6$  in a 50:50 (by volume) mixture of ethylene carbonate (EC) and dimethylcarbonate (DMC) was used as the electrolyte. Each cell was assembled in an argon-filled glove box, and electrochemical measurements were carried out at  $30^\circ\text{C}$  initially with charging, using a TOSCAT-3100 (Toyo System) at a current density of  $46.7 \text{ mA}\cdot\text{g}^{-1}$  (corresponding to 0.04C for  $2e^-/\text{Li}_2\text{S}$ ) between 3.0 and 1.0 V, after a stepwise pre-cycling treatment involving increasing the charge and discharge capacity limits at  $50 \text{ mAh}\cdot\text{g}^{-1}$  intervals up to  $600 \text{ mAh}\cdot\text{g}^{-1}$  [15]. Cyclic voltammetry (CV) of the cell was also conducted in a voltage range of 1.0–3.0 V (vs.  $\text{Li}/\text{Li}^+$ ) using a potentiostat/galvanostat (Model 1400, Solartron Analytical) at a scan rate of  $0.037 \text{ mV}\cdot\text{s}^{-1}$ .

### 3. Results and discussion

As reported previously [15], sample SPS( $600^\circ\text{C}$ ) was grayish black, and changed to a black powder after milling for 8 h (sample MM(8 h);  $\text{Li}_8\text{FeS}_5$ ). Fig. 1 shows the XRD patterns of the mechanically milled samples after different milling times. Sample MM(0 h) (corresponding to SPS( $600^\circ\text{C}$ )) consisted of crystalline  $\text{Li}_2\text{S}$  and  $\text{Li}_2\text{FeS}_2$  in a molar ratio estimated to be 82:18 by X-ray Rietveld analysis [19] using the crystallographic data reported previously [25,26]. This is roughly consistent with the ratio of 75:25 anticipated from the chemical reaction



The lattice parameter of  $\text{Li}_2\text{S}$  in sample SPS( $600^\circ\text{C}$ ) was estimated to be  $a = 5.6988(2) \text{ \AA}$ , which is smaller than that of the pristine  $\text{Li}_2\text{S}$  powder ( $a = 5.7144(2) \text{ \AA}$ ) as well as the reported value ( $a = 5.7158(1) \text{ \AA}$ ) [25]. This can be explained by the partial substitution of the smaller  $\text{Fe}^{2+}$  ions ( $0.66 \text{ \AA}$ ) for  $\text{Li}^+$  ions ( $0.74 \text{ \AA}$ ) [27], which is consistent with the above-mentioned smaller estimated amounts of  $\text{Li}_2\text{FeS}_2$  (18 mol%); the pristine FeS and/or formed  $\text{Li}_2\text{FeS}_2$  were partly decomposed during the SPS and some  $\text{Fe}^{2+}$  ions might be incorporated into  $\text{Li}_2\text{S}$ . Shortly after commencing milling, the sample quickly converted to low-crystalline  $\text{Li}_2\text{S}$  (MM(0.5 h)), and the XRD patterns showed little changes thereafter (MM(1 h) to MM(8 h)). Although detailed structural changes were not detectable by XRD,  $\text{Li}_2\text{FeS}_2$  probably decomposed and/or

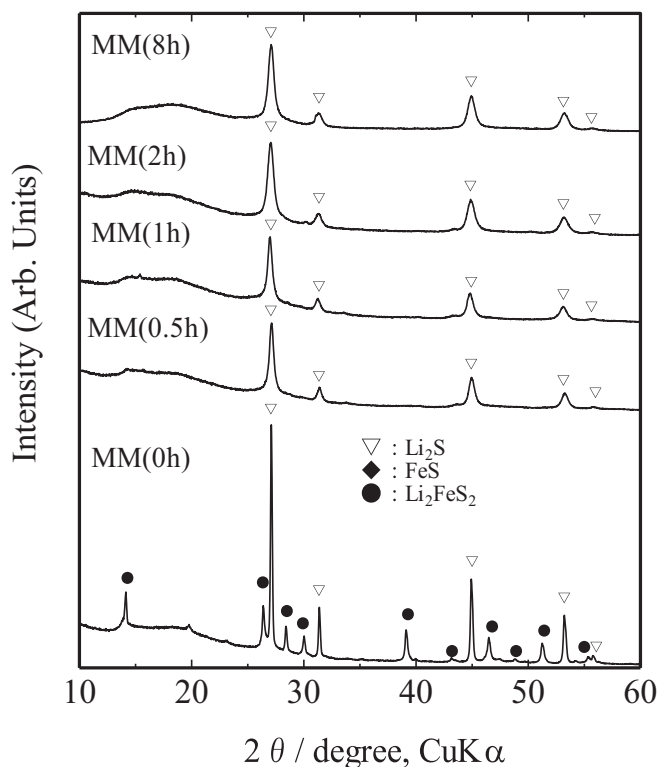


Fig. 1. XRD patterns ( $\text{Cu K}\alpha$  radiation) for samples MM(0 h) (corresponding to SPS( $600^\circ\text{C}$ )), MM(0.5 h), MM(1 h), MM(2 h), and MM(8 h) (corresponding to  $\text{Li}_8\text{FeS}_5$ ).

reacted with  $\text{Li}_2\text{S}$ , becoming incorporated into the low-crystalline  $\text{Li}_2\text{S}$  phase. The lattice parameter of sample MM(8 h) was estimated to be  $a = 5.7020(8) \text{ \AA}$ , which is smaller than that of the pristine  $\text{Li}_2\text{S}$ , and is consistent with the partial substitution of  $\text{Fe}^{2+}$  into  $\text{Li}_2\text{S}$ , as proposed above.

Fig. 2 shows typical SEM images of the MM samples after different milling times. After SPS treatment and before milling, the powder (MM(0 h)) consisted of relatively large grains, several to several tens of micrometers in size. After milling, the grain size was reduced, reaching a final size of less than  $2\text{--}3 \mu\text{m}$ . Notably the SEM image of sample MM(8 h) was similar to that of sample MM(2 h), suggesting that complete pulverization of the powder was nearly accomplished within 2 h.

To examine the local structure of the sample powder in detail, we carried out PDF analysis of the high-energy X-ray total scattering data, which is particularly useful for determining the structure of amorphous or low-crystalline samples [21–24]. First, we examined the local structure of sample SPS( $600^\circ\text{C}$ ) before milling. Fig. 3(a) shows the experimentally obtained X-ray PDF data (reduced pair distribution function  $G(r)$ ), which shows the probability of finding a pair of atoms, weighted by their scatter power, at distance  $r$  for sample SPS( $600^\circ\text{C}$ ) as well as those of the  $\text{Li}_2\text{S}$  and FeS starting powders. The PDF of sample SPS( $600^\circ\text{C}$ ) has a similar profile to that of the  $\text{Li}_2\text{S}$  powder, where specific peaks are attributable to interatomic distances in accordance with the reported crystallographic data [25], such as  $2.48 \text{ \AA}$  for S–Li,  $4.04 \text{ \AA}$  for S–S, and  $4.74 \text{ \AA}$  for second-neighbor S–Li interactions. These peaks shifted to shorter distances in sample SPS( $600^\circ\text{C}$ ), with the appearance of additional peaks at  $2.8$  and  $3.2 \text{ \AA}$ . This can be explained by (i) the coexistence of small amounts of  $\text{Li}_2\text{FeS}_2$ , whose interatomic distances calculated from reported crystallographic data [26] are also shown in Fig. 3(a), and/or (ii) partial substitution of smaller  $\text{Fe}^{2+}$  ions ( $0.66 \text{ \AA}$ ) for  $\text{Li}^+$  ions ( $0.74 \text{ \AA}$ ) [27] in  $\text{Li}_2\text{S}$ , as discussed above. Thus, the PDF data of sample SPS( $600^\circ\text{C}$ ) are consistent with the XRD results shown in Fig. 1, i.e., sample SPS( $600^\circ\text{C}$ ) consisted of partially Fe-substituted low-crystalline  $\text{Li}_2\text{S}$  and small amounts of  $\text{Li}_2\text{FeS}_2$ .

Download English Version:

<https://daneshyari.com/en/article/7744346>

Download Persian Version:

<https://daneshyari.com/article/7744346>

[Daneshyari.com](https://daneshyari.com)